Measurement of Mass and Beta-Lifetime of Stored Exotic Nuclei

Fritz Bosch

Gesellschaft für Schwerionenforschung (GSI), PO Box 64220, Darmstadt, Germany, f.bosch@gsi.de

Abstract. In this lecture, the basic techniques and concepts of ion storage-cooler rings are first presented, such as storing, beam-focusing and beam-cooling. In particular the main facets of electron cooling will be discussed, the cooling method being most successfully exploited in all operational ion storage-cooler rings. In the second part it will be demonstrated why and how an ion cooler-ring connected with a device producing exotic nuclei -as the coupled experimental storage ring (ESR) and fragment separator (FRS) at GSI in Darmstadt- is a unique tool to provide efficiently, precisely and with unrivalled sensitivity the ground-state properties of exotic nuclei, i.e. mass and (beta) lifetime. They are the basic and necessary ingredients for redrawing the pathways of stellar nucleosynthesis in the s-, rp- and r-processes, and also for exploring the limits of nuclear stability at both the proton and the neutron drip line, which directly reflects the deep entanglement of nuclear astrophysics on the one hand and of nuclear structure on the other. The two complementary methods of mass measurements, 'Schottky mass spectrometry' for longer-lived and 'isochronous mass spectrometry' for short-lived exotic nuclei, are visualized by plenty of data. Both methods were first developed and successfully applied at the ESR. In the last part of the lecture the unique worldwide potential of the ESR is demonstrated, namely the measurement of beta decays of highly-charged exotic ions, including the first observation of bound-state beta decay. This exotic mode of beta decay, being marginal for neutral atoms, becomes important in hot stellar plasmas during nucleosynthesis. As a striking example the impact of bound-state beta decay for the nuclear 'eon clock' ^{187}Re/^{187}Os and, connected therewith, for the determination of the age of our milky way galaxy and of the universe will be outlined.

1 Introduction

Beams of exotic ions are powerful tools to reveal the limits of nuclear stability in both the proton-rich and neutron-rich regime, to investigate nuclear structure at extreme neutron-to-proton ratios, and to redraw the various paths of stellar nucleosynthesis. For these purposes first of all the ground-state properties, mass and lifetime, of appropriate exotic nuclei are needed, because they provide key information on nuclear stability and determine the pathways of stellar nucleosynthesis and, therewith, the abundance distribution of the elements.

Over the last decade, ion storage rings have been proven to be ideally suited for precision experiments in the fields of atomic and nuclear physics.

F. Bosch, Measurement of Mass and Beta-Lifetime of Stored Exotic Nuclei, Lect. Notes Phys. **651**, 137–168 (2004)
http://www.springerlink.com/

To date, however, only one of these rings, the experimental storage ring ESR at GSI [1], can be fed also by *exotic* nuclei that are produced in a fragment separator (FRS, [2]) by in-flight fragmentation. It turned out that at the ESR masses and lifetimes of such fragments can be measured efficiently, precisely and with ultimate sensitivity, if applying sophisticated beam-cooling techniques (Sect. 2) either or special ion-optical modes (Sect. 3). Why those simple technical 'tools' can pave the way to a widely unexplored field?

The revolution time of an ion, stored in a ring with fixed magnetic rigidity Bρ, depends on its momentum–to–charge ratio mv/q. Because all kinds of 'cooling' techniques reduce the velocity spread of the stored ions to almost zero, the revolution frequencies of *cooled* ions solely depend on their mass-to charge ratio m/q. By measuring these frequencies, even small mass differences may be resolved. This technique, called 'Schottky mass spectrometry', will be presented in Sect. 3 together with the rich harvest collected in a few experiments only. Since cooling needs some time, which is at least in the order of a few seconds, the exploration of masses of short-lived nuclei cannot be addressed by this Schottky method and demands, therefore, another technique. For this purpose, at GSI the 'isochronous mass spectrometry' has been developed and successfully applied, based on a properly adjusted ion-optical mode, where the revolution time of a stored ion does *not* depend (in first order) on its velocity but only on its mass and charge. First results concerning the measurement of masses of short-lived, proton-rich nuclei are shown in Sect. 3.

Longer-lived, cooled exotic ions in a high atomic charge state can be stored for extended periods of time, i.e. up to many hours, depending on nuclear charge and on composition and pressure of the residual gas in the storage ring. A unique feature is that during storage the (high) atomic charge state of the ions remains well-preserved. Therefore, special β decay modes of *highly charged* exotic ions, such as bound-state β^- decay, have become accessible for the first time at the ESR. Bound-state β^- decay, the time-mirrored process of orbital electron capture (EC), is almost irrelevant in neutral atoms. However, becoming a significant decay branch for highly charged ions as prevailing in a hot stellar plasma, it can modify dramatically β lifetimes and even influence the pathways of stellar nucleosynthesis. In Sect. 4 examples of bound-state β^- decay are presented, with emphasis given to its crucial impact on the clockwork of nuclear 'eon clocks'.

2 Basics of Ion Storage-Cooler Rings

2.1 Hill's Equations, Betatron Oscillations, Tunes, and Space-Charge Limits

To store ions one needs a set of bending and focusing magnetic multipoles, a 'lattice'. Due to their finite horizontal and vertical emittances $\epsilon_{h,v}$, ions move

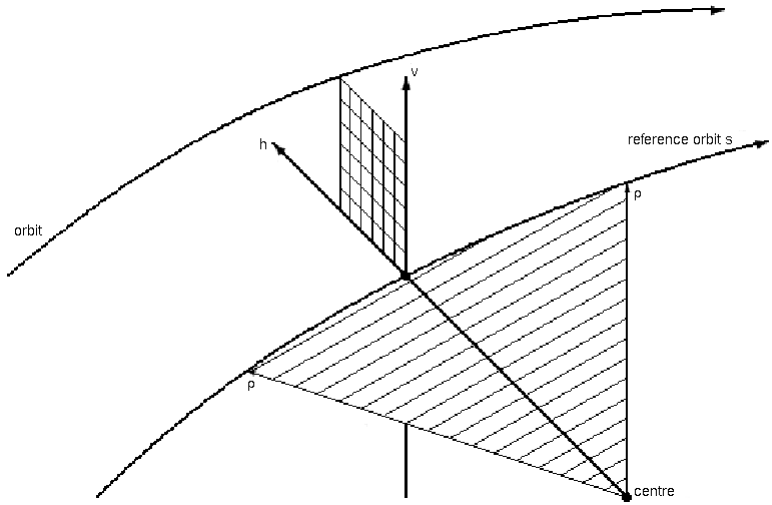

Fig. 1. Coordinates as used in (1) and (2) describing the motion of stored ions with respect to the reference orbit.

on quasi-periodic orbits, performing horizontal and vertical *'betatron oscillations'* with wavelengths $[\lambda_\beta]_{h,v}$ around the 'reference orbit' or 'Sollbahn'. The ratio of the orbit length C and the corresponding betatron wavelengths, $C/[\lambda_\beta]_{h,v} = Q_{h,v}$, is called the horizontal and vertical 'tune', $Q_{h,v}$, respectively. The orbits in terms of horizontal and vertical deviations from the 'Sollbahn' (including 'dispersion' due to finite horizontal and vertical momentum spreads $\Delta p_{h,v} \neq 0$) are solutions of Hill's differential equations [3], first proposed by Hill in 1886 to describe the motion of planets disturbed by three-body forces. In this curvilinear reference system s the amplitudes $u_{h,v}$ can be treated as two independent quasi-harmonic oscillations around s (see Fig. 1), according to:

$$d^2u\,(s)_{h,v}\,/ds^2 + k\,(s)_{h,v}\,u\,(s)_{h,v} - 1/\rho\;\Delta p_{h,v}/p_{h,v} = 0 \qquad (1)$$

where $u\,(s)_{h,v}$ denotes the deviations from the reference orbit s along moving horizontal and vertical axes, respectively, $k\,(s)_{h,v} = k\,(s+C)_{h,v}$ are periodic forces determined by the lattice design, ρ is the (mean) bending radius of the ring.

For a motion without dispersion ($\Delta p_{h,v} = 0$) 'cosine-like' solutions of (1) can be found defining the envelope of the ion motion in the given lattice:

$$u\,(s)_{h,v} = \{\varepsilon_{h,v}\beta_{h,v}\,(s)\}^{1/2}\cos\left\{\psi\,(s)_{h,v} + \delta_{h,v}\right\} \qquad (2)$$

with generalized 'phases' $\psi\,(s)_{h,v} = \int_0^C ds'/\beta\,(s')_{hv}$, and an arbitrary phase $\delta_{h,v}$. For this dispersion-free case the 'betatron amplitudes' $\beta(s)$ are determined only by $k(s)$, i.e. by the ring lattice. Strong focusing generates small

betatron amplitudes and, hence, large phases ψ(s). In this context the betatron wavelengths $[\lambda_\beta]_{h,v}$ and, therewith, the tunes $Q_{h,v}$ are defined as:

$$[\lambda_\beta]_{h,v} \equiv 2\pi C/\psi\,(s=C)_{h,v}\;;\; Q_{h,v} \equiv C/\,[\lambda_\beta]_{h,v} = \psi\,(s=C)_{h,v}\,/2\pi \qquad (3)$$

Integer (n) or 'algebraic' (m/n) numbers of the tunes lead to a resonance-like enhancement of small perturbations and an immediate loss of the stored beam. Therefore, the 'operating point' of a storage ring, the set of both horizontal and vertical tune, has to be chosen most carefully, i.e. as far as possible separated from all disturbing Q-resonances. Ion storage rings (see Fig. 2) accept emittances of typically $\epsilon_h = \epsilon_v = 10...30\ \pi$ mm mrad. Ions, such as those injected from a synchrotron, exhibit relative small longitudinal and transverse momentum spreads of typically Δp/p = 10^{-2} ... 10^{-3}, whereas 'hot', beams of exotic ions, delivered e.g. by a fragment separator, show momentum spreads up to a few percent. The latter determine, together with the lattice parameters Bρ and k(s), the solution of Hill's equations including dispersion, i.e. the actual betatron wavelengths, the betatron amplitudes and the tunes.

It is interesting to note that most probably the same mechanism of a 'Q-resonance' destroyed a former planet orbiting between Jupiter and Mars, due to its periodic encounter with Jupiter, and created what is now called the asteroid belt. Moreover, still today there exist many gaps (e.g. the famous 'Hecuba gap' [4]), where stable trajectories of asteroids cannot survive. This impressive similarity of effects governing the motion of celestial objects in a gravitation potential on the one hand, and of ions in a periodic lattice on the other hand, gets less astonishing if one remembers their common physics origin.

The tunes depend on the ion velocity, the ion number and on their momentum spread. When accelerating or decelerating stored ions, e.g. by rf-devices installed in the ring, one has to take care to cross the Q-resonances as fast as possible for avoiding significant beam losses. Coulomb repulsion between the ions with atomic charge q leads to a tune shift ΔQ which restricts the number of ions that can be stored. The corresponding maximum number of stored ions, N_{max}, the 'space charge limit', amounts, for vanishing momentum spread Δp, to:

$$N_{max} < \pi/r\; A/q^2\; \beta^2\gamma^3\; \epsilon_-\; [1 + (\epsilon_+ Q_-/\epsilon_- Q_+)]^{1/2}\; \Delta Q \qquad (4)$$

with the classical proton radius $r = e^2/\left(M_p c^2\right) = 1.5 \cdot 10^{-18}$ m, the atomic mass number A, the Lorentz factor $\gamma = \left(1-\beta^2\right)^{-1/2}$, the ion velocity β in terms of light velocity, and the larger (smaller) values of emittances and tunes, $\epsilon_{+/-}$ and $Q_{+/-}$, respectively. The tune shift ΔQ should remain smaller than about 0.2 to allow stable operation. One should also note the strong dependence of N_{max} on both the atomic charge state q $\left(\propto 1/q^2\right)$ and the ion velocity $\left(\propto \beta^2\gamma^3\right)$. In reality, the non-vanishing momentum spread ('chro-

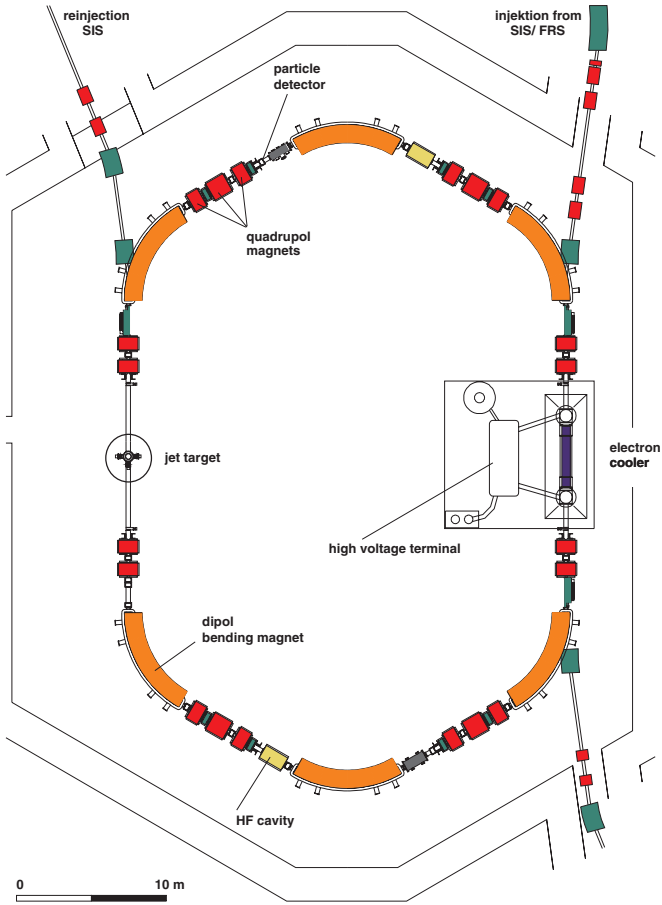

Fig. 2. The experimental storage ring ESR at GSI. The lattice of this ring shows a four-fold symmetry. The main installations are: six bending dipole magnets; several quadrupole duplets or triplets and some hexapoles for beam focusing; two rf cavities to bunch, accelerate and decelerate the beam; the electron cooler (middle of r.h.s.) to enhance the phase-space density; an internal, window-less (gas) target (middle of 1.h.s) and, not indicated, Schottky pick-up plates as well as pick-up and kicker for stochastic cooling.

maticity') further restricts N_{max} considerably. Some examples for bare, *uncooled* ions in the ESR are listed below, with $Q_+ = Q_- = 2.43$, $\Delta Q = 0.05$, and $\epsilon_{+-} = 1\pi$ mm mrad:

Ne^{10+}, E = 50 AMeV: $N_{max} = 1.9 \times 10^{13}$
Ne^{10+}, E = 500 AMeV: $N_{max} = 3.4 \times 10^{14}$

U^{92+}, E = 50 AMeV: $N_{max} = 2.2 \times 10^{11}$
U^{92+}, E = 500 AMeV: $N_{max} = 4 \times 10^{12}$

Electron cooling (see next section) that lowers the emittances ϵ by about one order of magnitude ($\epsilon \approx 0.1\pi$ mm mrad), reduces the above mentioned values of N_{max} by the same amount.

2.2 Beam Cooling

Ion beams injected into a storage ring have intrinsic horizontal and vertical emittances ϵ, defined as product of beam size and angular divergence or of beam size and transverse momentum. At constant energy these emittances are fixed, due to Liouville's theorem [5], when applying conservative forces only. The action of focussing a beam, for instance, reduces its size, but at the expense of enlarged angular divergence (transverse momentum). The area of the phase-space ellipse – the emittance – always stays constant. The only way to reduce *both* size and momentum spread, i.e. to enhance the phase-space density, is to let the beam interact with non-Liouvillian devices, by using non-conservative forces. This is called 'beam cooling'. Three cooling techniques have been successfully applied until now to cool stored, fast ions: stochastic-, electron-, and laser-cooling.

Laser cooling [6] which has been first proposed by Haensch and Schawlow in the seventies of the last century, is the key to bring neutral atoms to rest. To date, the most famous examples of laser cooling are magneto-optical traps, where Bose Einstein condensation has been achieved for the first time [7]. The basic idea of laser cooling is a directed momentum transfer $\Delta p = E_\gamma/c$ onto an atom by resonant absorption of a laser photon E_γ by a bound electron, followed by isotropic re-emission of the photon. From the momentum balance a net momentum transfer on the atom in direction of the laser beam arises. This effect can be used to narrow the longitudinal velocity profile of stored, fast moving ions by means of two tunable lasers: One of them, co-propagating to the ions, pushes their velocities to higher values, whereas a second counter-propagating laser pushes them back. By exploiting the considerable red- and blue-shifts, respectively, of the laser wavelengths seen in the ion rest frame, a very fast and efficient longitudinal cooling can be obtained. Laser cooling of stored fast ions has first been achieved at the test storage ring (TSR) in Heidelberg and almost simultaneously at the ASTRID facility in Aarhus [8]. Because laser cooling is based on rather small electron excitation energies, it is restricted to moderately charged ions with appropriate electronic structures as, e.g. Be^+ or metastable Li^+. For highly charged ions it cannot be applied, except for a few cases of H-like or Li-like ions, where the condition of matching the electronic structure is fulfilled due to the hyperfine splitting of the ground state [9].

In contrast to laser cooling, stochastic as well as electron cooling are universal methods to cool all kinds of fast ions in both longitudinal and transverse directions. Stochastic cooling has been developed by van der Meer [10] at CERN at the end of the seventies. At that time stochastic cooling was the only way to cool hot antiprotons and to prepare them for injection into

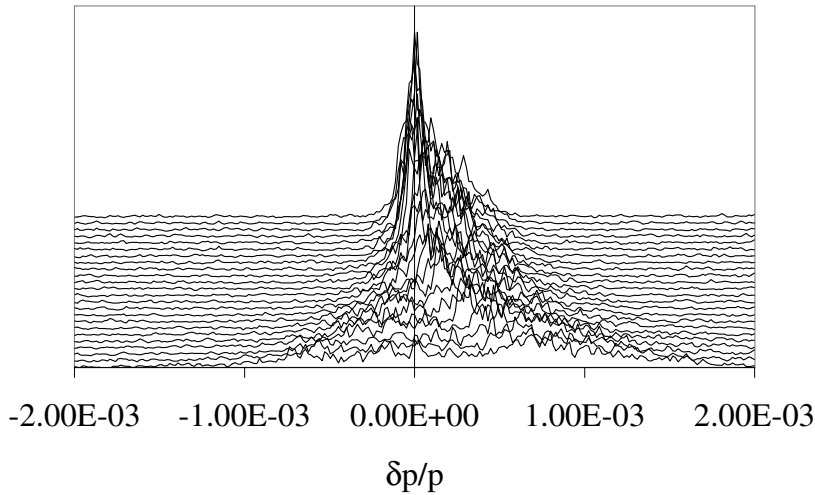

Fig. 3. Time development of momentum spread δp/p of some 10^5 'hot' ^{40}Ar ions in the course of stochastic cooling, recorded every 100 ms. Courtesy of M. Steck [12].

the proton-antiproton collider at CERN, which has led to the detection of the W^+ and W^- vectorbosons, the mediators of weak interaction.

Stochastic cooling is a kind of 'self-correction' of the ion beam. A couple of plates (pick-up electrodes) registers deviations of the ions from the 'Sollbahn' as a difference of the signals induced onto the right and left plate, respectively. The signals, recorded over a large bandwidth of typically some 100 MHz and amplified, are used to correct the ion motion within the *same* turn, at a location ('kicker') that is exactly (n + 1/4) betatron wavelengths apart from the pick up, that is at a zero crossing of the betatron oscillation. This technique fits to one specific ion velocity only and demands, furthermore, a very fast amplification. Though the correction signal is appropriate for some ions but wrong for other ones, it can be shown that within a short time (typically 1 s for heavy ions) the average phase-space volume of the ion ensemble will be significantly reduced.

Since stochastic cooling is most effective for 'hot' beams ($\Delta p/p \geq 10^{-3}$... 10^{-2}), it may serve as an ideal tool for pre-cooling, followed by electron cooling which is much less suited for this regime of large momentum spreads. Very recently stochastic and electron cooling of hot fragments could be combined successfully at the ESR [11], which reduced the overall cooling time to a few seconds only (see Fig. 3).

Electron cooling has been invented in the sixties of the last century by Budker [13] in Novosibirsk and first realized there [14]. To date it is the most widely applied cooling scheme, installed at almost all ion storage rings. It relies upon momentum exchange by Coulomb collisions between hot ions

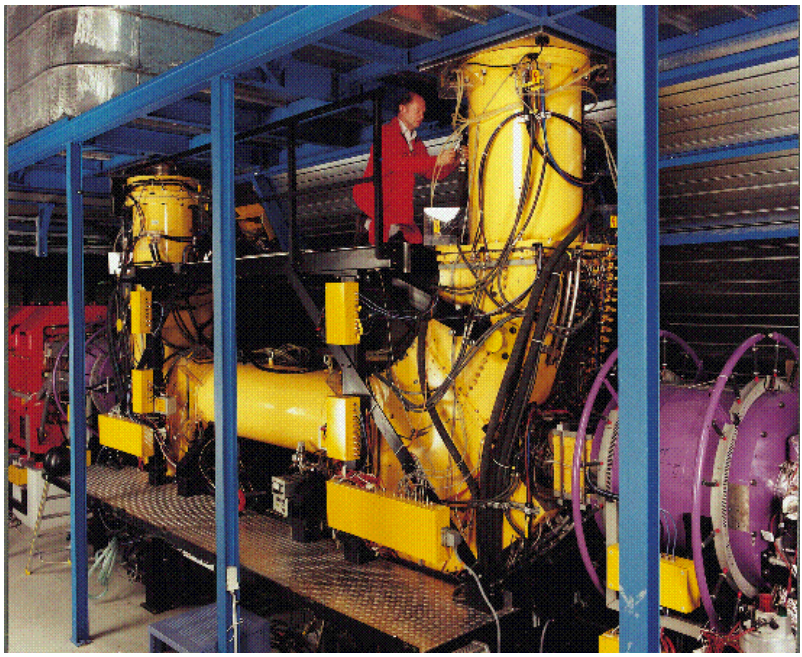

Fig. 4. Electron cooler at the ESR. The electrons have almost the same mean velocity as the ions but a much smaller velocity spread. The ion beam comes from bottom right, the electrons from top right, smoothly guided to and extracted from the common interaction zone (length about two meters) by a toroidal magnetic field. The ions come back after one turn of about 500 ns duration to interact anew with 'fresh' electrons. Along this region a longitudinal magnetic field of typically 0.05 T confines the electrons.

and collinear, cold electrons that are radially confined by a magnetic field of typically 0.01...0.1 T (Fig. 4). After one interaction cycle (ions and electrons move in parallel for about a few meters) the electrons are extracted by a weak toroidal magnetic field, whereas the 'old' ions come back after their next turn to interact anew with fresh, cold electrons. Due to this ingenuous 'trick', thermal equilibrium is reached within a short time, leading to an assimilation of both the longitudinal (T_l) and transverse (T_t) temperatures of electrons and ions, according to [15]:

$$\begin{aligned} kT_l &= A\beta^2 c^2 (\Delta p/p)_e^2 \\ kT_t &= 1/2A\,\gamma^2\beta^2 c^2\,(\epsilon_h/\beta + \epsilon_v/\beta)_e \end{aligned} \tag{5}$$

According to (5) the transverse equilibrium temperature T_t gets proportional to the horizontal and vertical emittances of the electron beam which, on their part, are determined mainly by the cathode temperature (about 1200 K). Thus, kT_t-values of about 100 meV are routinely obtained. This can be improved by more than an order of magnitude by exploiting the technique

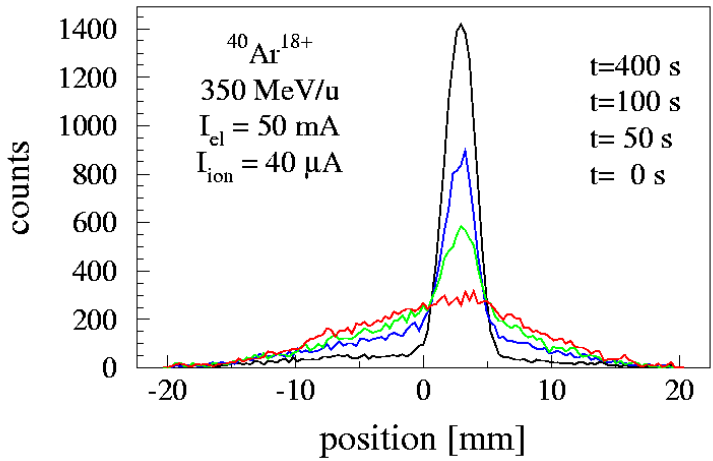

Fig. 5. Time development of electron cooling for 8 x 10^6 bare ^{40}Ar ions, mirrored by the size of the stored beam. To get a more detailed information, the usual electron current $I_{e\ell}$ of several hundred mA has been reduced to 50 mA, yielding a much enlarged cooling time. Courtesy of M. Steck [12].

of 'adiabatic expansion' of the magnetic field between cathode and interaction region, first introduced by Danared [16] at the CRYRING in Stockholm. For high ion velocities ($\beta \geq 0.1$) the longitudinal temperatures kT_ℓ get much smaller than kT_t, due to the relativistic shrinking of the electron momentum spread $(\Delta \mathrm{p/p})_e$ after acceleration.

The cooling time τ_c scales according to [15]:

$$\tau_c \propto A/Z^2 \, 1/j_e \, |\Delta v|^3 \tag{6}$$

where A and Z are the atomic mass and nuclear charge of the ions, respectively, j_e the electron current and Δv the halfwidths of the ion velocity distribution in the electron rest frame. Therefore, electron cooling is fastest for very heavy ions and small velocity spreads.

Since the cooling time is proportional to the cube of the relative velocity spread, electron cooling ist most effective if rather 'cold' ions are injected, e.g. directly from a synchrotron. In this case cooling times of below one second can be easily obtained. For instance, with A = 200, Z = 80 (lead region), j_e = 200 mA and $\Delta \mathrm{v/v} = 10^{-3}$, τ_c amounts to about 0.2 s. On the other hand, for unstable hot fragments with typical relative velocity spreads near to or even above 10^{-2}, τ_c steeply rises to about 10...30 s. Hence, for the observation of electron-cooled short-lived fragments stochastic pre-cooling is mandatory.

Electron cooling provides brillant beams of small size (typically 2 mm for 10^6 stored ions) and small momentum spread ($\Delta \mathrm{p/p} = 10^{-6}...10^{-7}$), depending on the number of ions (Fig. 5). At ion numbers of a few thousand even a phase transition to an ordered linear ion chain has been observed

[17], where the momentum spread is solely due to the stochastic (small) fluctuations of the magnetic fields of the lattice.

Storage times are defined as the decrease of the initial number of ions to a 1/e-level. Values of many hours for light ions such as C, Ne, Ar and of about one hour for heavy, highly charged ions like Pb or U can be achieved routinely at a residual gas pressure of about 10^{-11} mbar with all ions revolving at the *same* velocity. This most important result of electron cooling, i.e. the common velocity of all ions, is the basis of 'Schottky mass spectrometry' to be presented in the next section. On the other hand, the rather long times needed for electron cooling prevent its application to mass- and lifetime measurements of short-lived exotic nuclei with half-lives significantly less than one second (even if combining stochastic pre-cooling and electron cooling).

3 Mass Measurement of Stored Exotic Nuclei – 'Schottky'- and 'Isochronous' Mass Spectrometry

Protons and neutrons are the constituents of the atomic nucleus which is, on its part, the core of the atoms, the building blocks of all chemical elements that we encounter in the universe. One important task of nuclear physics is to understand the existence, the structure and the limits of nuclear matter in terms of the interaction of protons and neutrons and of the well-balanced symmetry between them. In the past, nuclear research was constrained essentially to a narrow band of nuclei around those of natural abundance. The existence of nuclei with a different composition of their constituents supposes, however, that their proton-to-neutron ratio stays within certain limits, the 'drip lines'. Approaching these borderlines of nuclear stability is one of the big challenges of present nuclear structure research. The installation and operation of exotic-nuclear-beam facilities all over the world during the past decade brought a major step into this direction, by providing for the first time nuclei far from stability that exhibit a pronounced asymmetry of protons or neutrons, respectively.

Exploring the limits of nuclear stability is, however, indissolubly intertwined with one of the key questions of nuclear astrophysics, namely the creation of the heavy elements in stars. This twin-aspect will be addressed continuously in the forthcoming sections, by emphasizing in particular the key-role of masses and β lifetimes for the limits of nuclear stability as well as for the pathways of stellar nucleosynthesis. Techniques developed at GSI will be presented to produce proton-rich nuclei far from stability by in-flight fragmentation, to store and to cool them in the experimental storage ring ESR, and to determine their fundamental properties, mass and lifetime, by two complementary methods, named 'Schottky' and 'isochronous' spectrometry, respectively. The results shown will demonstrate convincingly the unsurpassed effectivity, the high mass resolving-power, and the ultimate sensitivity of these two techniques. Finally, it will be outlined, how the present

limits of Schottky spectrometry, concerning its restricted time-range, could be improved and how in future experiments also neutron-rich nuclei far from stability might be addressed.

3.1 The Deep Entanglement of Nuclear Structure and Stellar Nucleosynthesis

All atomic nuclei in the universe beyond lithium have been and still are being created in stars [18]. In various stellar environments this nucleosynthesis proceeds via the formation of transient nuclei that decay into stable ones, either directly or after several intermediate steps. The remnants of these processes, dispersed from dying stars into the interstellar space, eventually contract and serve as the seeds for a new generation of stars and their companions, such as our sun and the earth. We all are literally made out of the dust of stars. Understanding the formation, evolution and final fate of the stars as well as revealing stellar sites, pathways and time scales of the stellar synthesis of the elements can be achieved, however, only within the closest connection of astrophysics and nuclear physics (Fig. 6). Whereas the former defines feasible stellar scenarios in terms of temperature, density, pressure and chemical composition, the latter may supply fundamental characteristics, such as masses and lifetimes, of some key-nuclei that are transiently created and destroyed again during the many complex steps of nucleosynthesis.

Hence, astrophysics and nuclear physics appear deeply intertwined: because stellar scenarios might depend on nuclear structure and, vice versa, nuclear properties might be altered in different stellar environments, the real pathways of nuclear matter creation can be redrawn only via a most careful synopsis of both of them, and after many iterative steps that include experimental data as well as theoretical modelling.

Light and medium-heavy elements are produced by nuclear fusion in the hot and dense core of stars. After a long-lasting burning of hydrogen into helium, heavier and heavier nuclei are formed by subsequent fusion processes. Nuclear fusion ceases not later than at iron, because there any additional fusion would require input of energy. As a result, small- (like our sun) and medium-sized stars burn out at latest when this stage has been reached. Only in very mass-rich stars the creation of heavy atomic nuclei proceeds further on the neutron-rich side, by the interplay of neutron capture and of α-decay. The stable, heavy and neutron-rich atomic nuclei found in our solar system have been produced in at least two processes, as it was concluded from their abundances. One of them, the slow neutron capture process ('s-process'), creating nuclei close to the valley of β-stability, is believed to be generally understood [19]. However, most of the heavy nuclei, such as uranium and thorium, originate from an explosive process of nucleosynthesis, the so-called rapid neutron capture ('r-process'). Although at the time being, the outbreak of Supernovae of type II or the merger of neutron stars are favored, the true

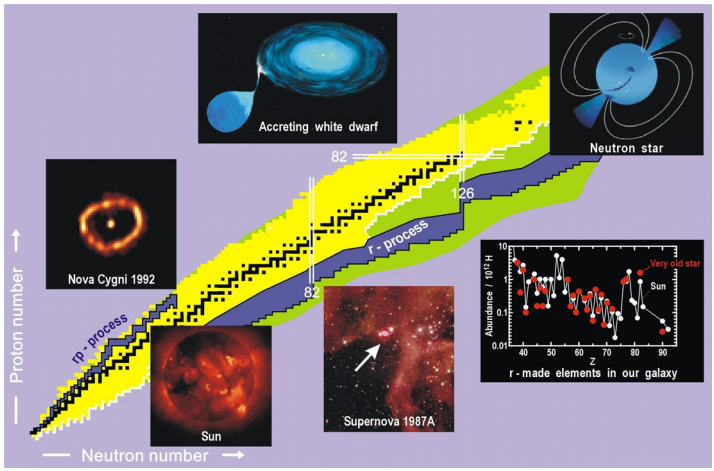

Fig. 6. Nuclear astrophysics is seeking, in closest connection with nuclear structure research and based on key-properties of unstable nuclei, for a reliable description of the various kinds of stellar nucleosynthesis. One of its major aims is to understand the abundance-distribution of the elements in the universe. Some of the presumed scenarios of matter creation in stars are: nuclear fusion up to iron, e.g. in the sun; explosive rapid neutron capture (r-process), going on perhaps in the outbreak of Supernovae of type II like the Supernova 1987A; rapid proton capture (rp-process), occurring in Novae explosions of accreting white dwarfs like Nova Cygni 1992, or in X ray bursts emerging from accreting neutron stars. The remnants of a Supernova might become a fast-rotating neutron star with degenerate, ultra-dense nuclear matter.

stellar site of the r-process is still unknown [20]. As well its pathway is widely hidden, due to a lack of appropriate nuclear data in this regime.

Neutron-deficient nuclei close to the proton 'drip line' are produced in other explosive scenarios, as signaled by Novae explosions of 'white dwarfs' that pick up additional mass, or by X ray bursts probably emerging from the surface of growing neutron stars. In these processes, hydrogen is explosively burnt via a sequence of rapid proton captures ('rp-process') and β^+ decays close to the proton drip line. However, similarly to the r-process, many of the questions related to the rp-process have not yet been answered [21].

In particular the explosive, cataclysmic processes of stellar nucleosynthesis are for the most part not yet understood, including also the specific properties of their remnants, such as neutron stars [22]. To shed light into this scarcely explored field, experiments based on exotic nuclear beams are needed which can provide the fundamental properties of nuclei far from stability. Among them, nuclear masses and lifetimes are by far the most important ones: the nuclear masses, because they 'contain' the sum of all strong interactions and determine, therefore, the pathway itself of the r- and rp-processes; the β lifetimes, because they finally generate the abundance pattern accumulated along these paths of nucleosynthesis.

Obviously those data are urgently needed: the abundance of r-made elements as found in our solar system does not fit to a simple extrapolation of the shell structure of stable nuclei into a region with large neutron excess. Instead, a significant softening of the shell gaps with increasing neutron number has to be presumed [23]. To make this conjecture a matter of fact, demands, first of all, the knowledge of the masses and lifetimes of the corresponding neutron-rich nuclei. Moreover, as data from very old stars of the galactic halo suggest, there might be even a second pattern of r-made medium-heavy elements which is not observed in the elemental distribution of the sun (see inset of Fig. 6). Also this presumption can be confirmed or disproved only by corresponding nuclear data, in particular masses and lifetimes, in connection with an appropriate stellar model. All this corroborates the indissoluble linkage of the basic properties of nuclei far from stability on the one hand, and of the creation of matter in explosive nucleosynthesis on the other hand. They are the two sides of *one* medal.

3.2 In-Flight Production, Storage and Cooling of Exotic Nuclei at the GSI Fragment Separator and Storage Ring

At GSI a new generation of experiments on radioactive nuclei has been pioneered by a unique combination of a heavy ion synchrotron SIS, a fragment separator FRS [2] and an experimental storage ring ESR [1] as shown in Fig. 7. Stable-isotope ions, accelerated in the SIS to an energy of several hundred MeV/u, hit at the entrance of the fragment separator a production target, where exotic nuclei are produced by in-flight projectile fragmentation [24] (stripping of protons and/or neutrons from the primary ion). In the separator, which is operated as a magnetic achromat, fragments within a small band of magnetic rigidity Bρ are selected and transported to the storage ring.

In this way, exotic ions within the same band of magnetic rigidity Bρ, but dispersed over the entire range of the periodic table, are produced and simultaneously injected into the storage ring. If, however, in the first dispersive focal plane of the separator specially shaped degraders are placed, *one* single nuclear species can be singled out for injection into the storage ring, due to the nuclear charge dependent energy loss ΔE in the degrader (Bρ-ΔE-Bρ method) [25]. By in-flight fragmentation preferentially fragments at the proton-rich side of the nuclear chart are generated. Very recently, however, fission of relativistic uranium projectiles has been successfully applied to create and to store neutron-rich fragments close to the magic neutron shell N = 82 [26]. A unique feature of the SIS-FRS-ESR couple is the production and storage of *highly charged* exotic ions (mainly bare or hydrogen-like), due to the projectile fragmentation at high energies. Therewith for the first time β decays of exotic nuclei in a high atomic charge state can be addressed, i.e. under conditions similar to those prevailing in hot stellar plasmas during nucleosynthesis.

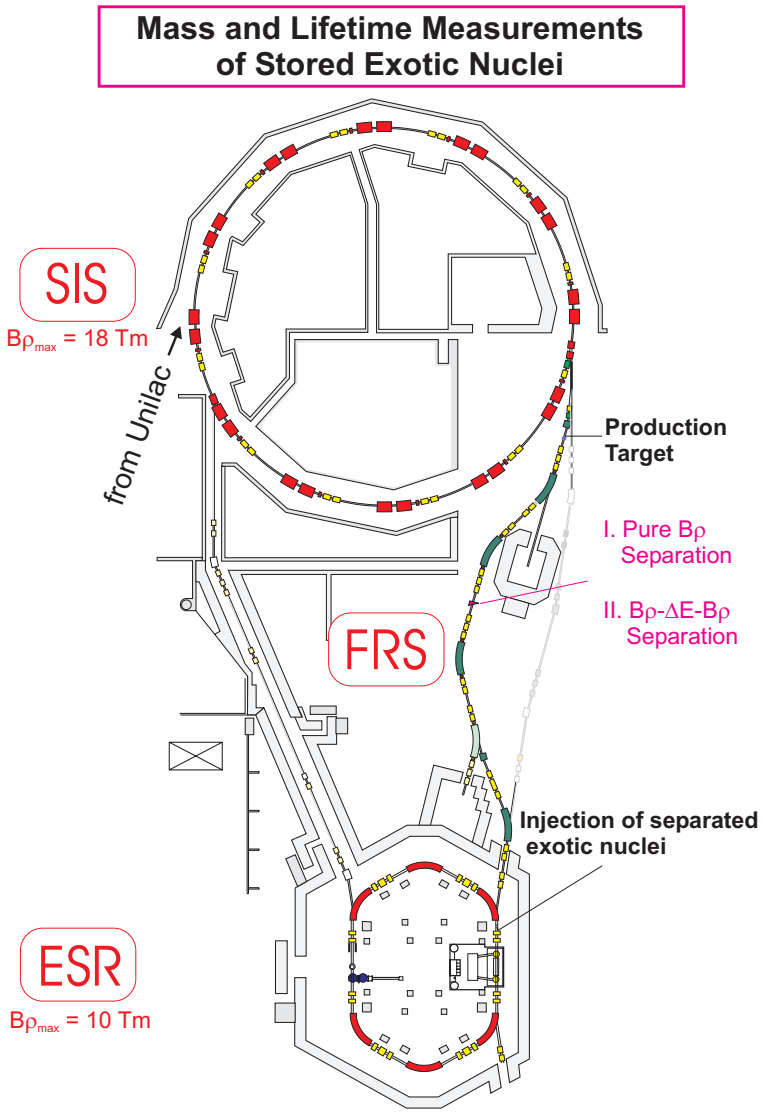

Fig. 7. The combination of the heavy ion synchrotron SIS, the fragment separator FRS and of the storage-cooler ring ESR for production, storage and cooling of exotic, highly charged ions.

The exotic beams accepted by and stored in the ESR are 'hot', i.e. their relative momentum spread $\Delta p/p$ is rather high (typically 10^{-2}), and their angular divergence and size are large. For most of the experiments presented in the following, first a 'beam cooling' is required. As discussed in Sect. 1, three cooling techniques have been successfully applied until now to cool

stored ions: stochastic-, electron-, and laser-cooling. For hot, exotic ions produced in the FRS and transferred to the ESR, electron-cooling times rise to more than about 10...30 s. Combined with stochastic pre-cooling, however, an overall cooling time of a few seconds for such ions can be achieved, as it has been demonstrated at GSI very recently [11]. By using this technique, which is called ''Schottky' mass spectrometry, and will be discussed next, can be extended in the near future onto exotic nuclei with half-lives below a few seconds.

3.3 'Schottky' and 'Isochronous' Mass-spectrometry of Exotic, Highly-Charged Ions

For two species of ions with velocities $v_1 = \beta_1 c$, $v_2 = \beta_2 c$ and mass-to-charge ratios $(m/q)_1$ and $(m/q)_2$, respectively, circulating in a storage ring with revolution frequencies f_1 and f_2, the following equation can be derived [27]:

$$\Delta f/f = -1/\gamma_t^2 \, \Delta(m/q)/(m/q) + \Delta v/v \, (1 - \gamma^2/\gamma_t^2) \qquad (7)$$

where f, m/q, v and γ are the corresponding mean values of frequency, mass-to-charge ratio, velocity and $\Delta f = f_1 - f_2$, $\Delta(m/q) = (m/q)_1 - (m/q)_2$, and $\Delta v = v_1 - v_2$, are the corresponding differences of frequency, mass-to-charge ratio and velocity, respectively; γ_t is the 'transition energy', at which the revolution frequency gets independent on the energy for each ion species with fixed m/q-ratio. This transition energy γ_t can be varied within certain limits by a careful choice of the ion optics of the storage ring.

An inspection of (7) shows that a one-to-one correspondence between the relative difference of revolution frequencies $\Delta f/f$ on the one hand, and the relative difference of the mass-to-charge ratios $\Delta(m/q)/(m/q)$ on the other hand, is established, if and only if the second term at the right hand side of (7) can be neglected. This can be achieved by two alternative methods, as shown in Fig. 8: either by getting rid of any velocity spread ($\Delta v \to 0$), or by operating the ring at the transition energy ($\gamma \to \gamma_t$). The former method is the basis of Schottky mass-spectrometry. It applies cooling, in particular electron cooling, to get a well-defined, sharp velocity for all stored ions. Because electron cooling of hot fragments needs a considerable time, this technique remains restricted to longer-lived exotic nuclei with half-lives above some seconds, as long as stochastic pre-cooling cannot be applied.

The second, 'isochronous' method, does not need any kind of cooling and is, therefore, suited in particular for short-lived ions. Here the hot ions are injected at the transition energy $\gamma = \gamma_t$, where the revolution time of a given ion species becomes (almost) independent on the velocity. Hence, both complementary methods can provide the mass-to-charge-ratios of all the stored ion species just by measuring their corresponding revolution frequencies. Of course, the frequency scale has to be calibrated in terms of the mass-to-charge ratios m/q, by means of appropriate ions of known mass and charge that are stored simultaneously.

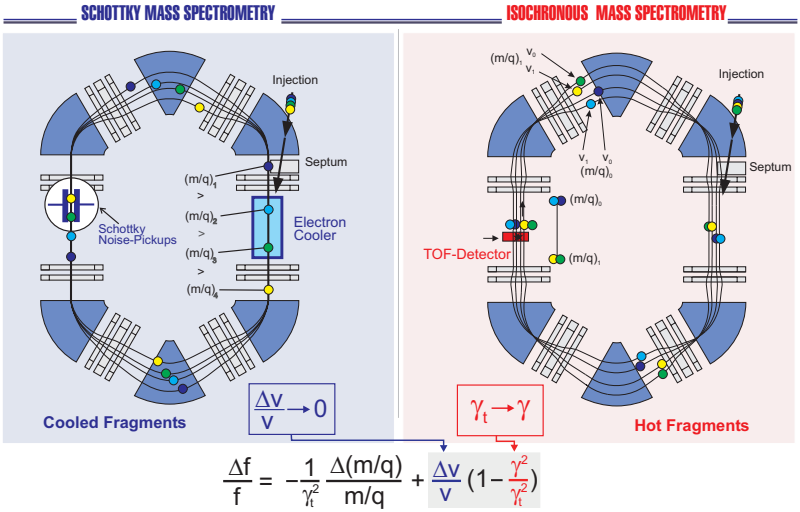

Fig. 8. The two kinds of mass spectrometry applied at the ESR by measuring the revolution frequencies of stored exotic ions. Left hand side: Schottky mass-spectrometry. Here the ions are electron-cooled, therefore their velocity spread Δv gets negligibly small. Their revolution frequencies are measured by pick up plates mounted in the ring aperture. This technique has been successfully applied at longer-lived exotic nuclei. Right hand side: Isochronous mass-spectrometry. Uncooled ions circulate at the transition energy γ_t. Their revolution times are measured by a time-of-flight technique. This method is in particular suited for short-lived nuclei with half-lives in the millisecond- or even microsecond range.

Schottky mass spectrometry. The stored, electron-cooled ions all have a common velocity imprinted by the cooler electrons and, thus, a negligibly small velocity spread Δv. Then, according to (7), a one-to-one correspondence between revolution frequency f_i and mass-to-charge ratio $(m/q)_i$ for each stored ion species exists. Every ion, q-times charged, induces at each passage a signal proportional to q^2 onto a couple of plates mounted in the ring aperture ('Schottky noise pick-up'). These signals are sampled, Fourier-transformed and mixed with a local oscillator to convert the original revolution frequencies into a frequency range of a few hundred kHz. In principle, all harmonics of the fundamental revolution frequency (typically 2 MHz) can be used for this purpose. A data acquisition system, 'time capture', combines a large bandwidth, wide enough to record the frequencies of all stored ions simultaneously, with a high resolution of a few Hz. An example of recent ESR data is shown in Fig. 9. The main panel of this figure shows a wealth of some fifty well-resolved, simultaneously recorded lines. A zoom into this spectrum displayed as inset demonstrates the high resolving power for the example of the well-resolved isomeric and ground state of ^{143}Sm, only 754 keV apart from each other, and also the capability of unambiguously detecting one single stored ion.

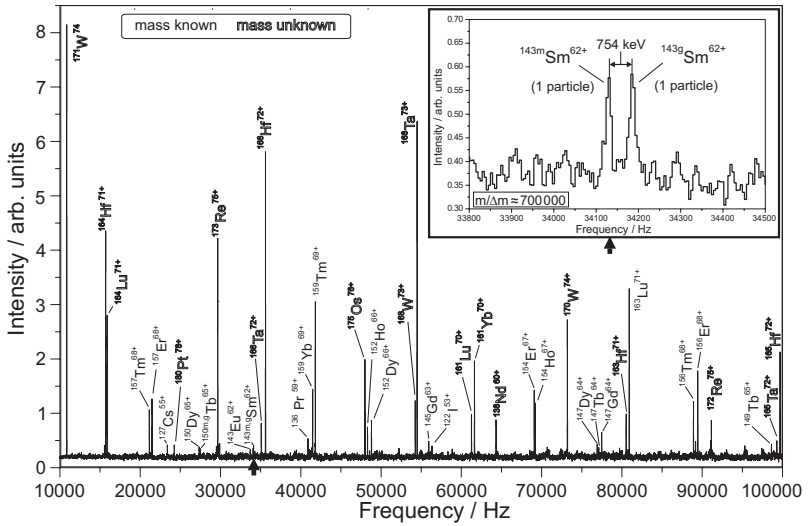

Fig. 9. Schottky spectrum of fragments from a primary ^{209}Bi beam, stored and electron-cooled in the ESR. The main spectrum shows the difference between the 30th harmonic of the revolution frequencies of the many stored ion species and of a local oscillator operating at about 60 MHz. It covers roughly the full acceptance of the ESR. The inset shows a zoom into the spectrum with the well-resolved ground and isomeric state of bare ^{143}Sm^{62+}, each of them populated by one single ion. Parts of this figure were originally published in [27,28].

Schottky mass spectrometry shows very specific and partially unique features. This technique offers a presently unsurpassed efficiency: about 50 masses can be determined *simultaneously*, i.e. with one filling of the storage ring, provided that appropriate nuclei with known masses are stored in the same 'package' for the purpose of calibration. The detection limit of *one single stored ion* (for nuclear charges Z $\geq$ 40) is impressive, indeed.

Although the mass resolving-power m/Δm of about 7 x 10^5, corresponding to an accuracy of about 100 keV for heavy nuclei, cannot compete with 'world record values' of 10^{10} accessible in ion traps, it is by far sufficient for a broad mass-mapping of exotic nuclei far from stability. Since the frequencies and thus the masses of neighbouring isobars multiplets, connected by β decay or electron capture, are measured simultaneously, the mass differences (Q values) of the corresponding parent and daughter nuclei can be determined 'on line'. For the time being, this opportunity to simultaneously perform a mass spectroscopy of isobars is unrivalled. However, Schottky mass spectrometry is presently restricted to rather long-lived exotic nuclei because of the time needed for electron cooling of hot fragments. If one could succeed to combine electron cooling with fast stochastic pre-cooling, mass measurements in a storage ring could be extended to nuclei with half-lives in the range of a second or even less.

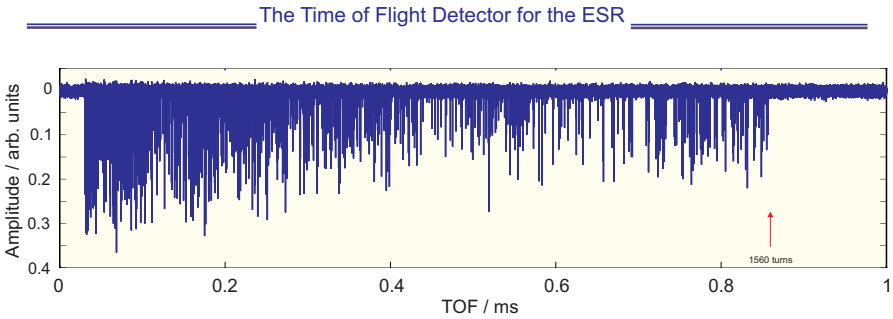

Fig. 10. Periodical 'fingerprints' in the TOF detector of a few ions stored at the transition energy γ_t. The maximum number of turns of one ion, as observed in this spectrum, amounts to 1560. This figure was originally published in [29].

Isochronous mass spectrometry. A complementary approach, in particular tailored for uncooled, short-lived nuclei very far from stability, is isochronous mass spectrometry at the transition energy, where the revolution frequency gets stationary for a given m/q-ratio. Here the revolution *times* of each individual stored ion are measured by a time-of-flight (TOF) technique. The ions cross a very thin, metallized carbon foil (a few μg/cm^2 thick) mounted in the ring aperture, and eject at each passage δ-electrons which are guided by electric and magnetic fields to a detector. Its fast-sampled signals represent the sum of all time-stamps of all ions, produced periodically by every ion at each passage. It is the task of a somewhat sophisticated software to assign this confusing manifold of 'fingerprints' (Fig. 10) to individual ions and to derive from it a frequency spectrum such as shown in Fig. 11. In spite of the energy loss in the foil, more than 1500 turns could be observed for one and the same ion.

Isochronous mass spectrometry, being restricted by obvious reasons to a small number (30...50) of simultaneously stored ions, is extremely well suited to address short-lived nuclei very far from stability that are produced with very small production cross-sections (microbarn...nanobarn) in projectile fragmentation or fission. The mass resolving power achieved in first experiments was near to 10^5, corresponding to an accuracy of a few 100 keV for medium-heavy nuclei. By this isochronous mass spectrometry one single stored ion can be easily detected, independent on its charge state. In principle, half-lives of only a few microseconds can be measured by this technique.

3.4 Summary of Schottky and Isochronous Mass Spectrometry

Figure 12 summarizes the harvest of four experiments addressing Schottky or isochronous mass spectrometry [27–31]. It reflects, first of all, the extremely attractive features of both methods which are almost unrivalled. In these four

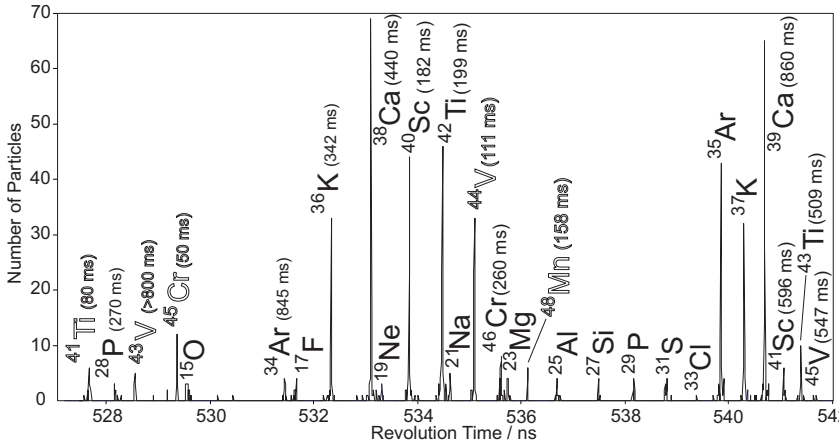

Fig. 11. Revolution time spectrum of fragments of a primary ^{52}Cr beam, taken by the TOF detector. Previously unknown masses are indicated by outlined letters. This figure was originally published in [28].

experiments more than 170 previously unknown masses were determined, that is about 8% of all nuclear masses ever measured. In all cases the mass resolving-power m/Δm was within 10^5 and 7 x 10^5, corresponding to an accuracy between 50 and a few hundred keV. The detection limit was one single ion for all ion species in case of the isochronous method, and one single ion for a charge state q $\geq$ 40 in the case of Schottky spectrometry.

The new masses are entirely restricted to the proton-rich side of the nuclear chart, as the technique of projectile fragmentation was applied. Thus, the proton drip line has been reached for nuclei above Z = 82. In some α-chains, only mass differences (Q values) were previously known. By measuring for the first time the masses of the corresponding endpoints of these chains, masses were derived also for all members of the chains [27,30]. Furthermore, some masses of short-lived light nuclei that are important for the rp-process were determined for the first time by the isochronous method [31].

4 Measurement of Beta-Lifetimes of Stored, Highly Charged Ions

The SIS-FRS-ESR facility has provided the very first opportunity to produce β-unstable, highly charged ions, to cool and store them for extended periods of time and to measure their lifetimes. The high atomic charge states deserve much more than academic interest, because they mirror the scenario occurring in hot stellar plasmas during nucleosynthesis. In the s-process, proceeding along the valley of β stability, the mean 'temperature' (kT) is around 30 keV, in the explosive r-process even above 100 keV [22]. Therefore, in both processes the mean atomic charge state <q> becomes high. The much

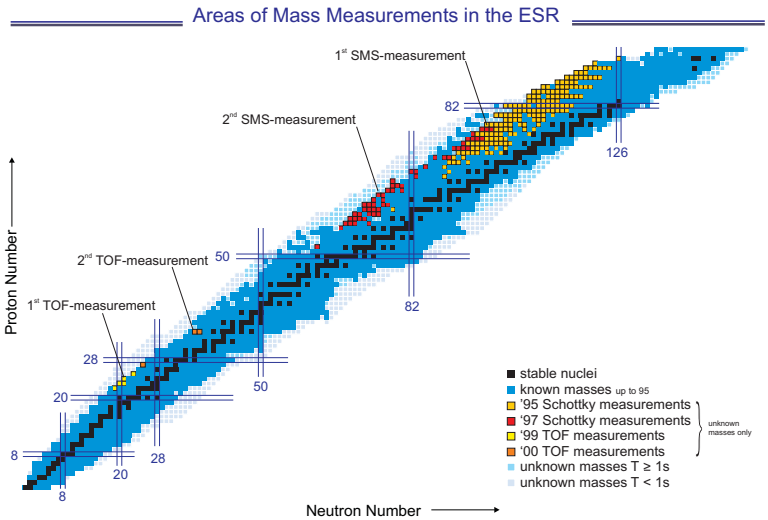

Fig. 12. The harvest of four experiments of Schottky (SMS) and isochronous (TOF) mass spectrometry. This figure was originally published in [27].

reduced number of bound electrons causes significant, sometimes even dramatic, changes of β lifetimes with respect to neutral atoms. The orbital EC decay probability — depending trivially on the number of bound electrons — is strongly reduced or even vanishes in case of bare ions. Bound-state β^- decay, where the newly created electron remains bound in a previously empty (inner) orbit of the daughter atom, becomes an important decay branch, in sharp contrast to neutral atoms. It was not surprising, therefore, that bound-state β^- decay could not be observed but after the ESR went into operation (see Sect. 4.2).

It is in principle very simple to measure a β lifetime of cooled, highly charged ions orbiting in a storage ring such as the ESR: one has just to record the areas of the Schottky lines of the parent and daughter ions as a function of time, because they are proportional to the corresponding particle numbers ('Schottky lifetime spectroscopy'). A unique feature of this method is that the time development of the number of the parent and daughter ions can be observed in principle *simultaneously*, in contrast to most other detection methods.

If the ions undergo a 'continuum' β decay (β^+, β^-), both the mass and the atomic charge state change, which causes a significant change of trajectory and revolution frequency of the daughter ion. This can be exploited either in the Schottky spectrum, or by means of particle detectors mounted at appropriate position in the ring aperture. Both complementary techniques provide a high detection efficiency and allow one to address β half-lives in the range from a few ms (particle detector) up to some 100 years. However, in

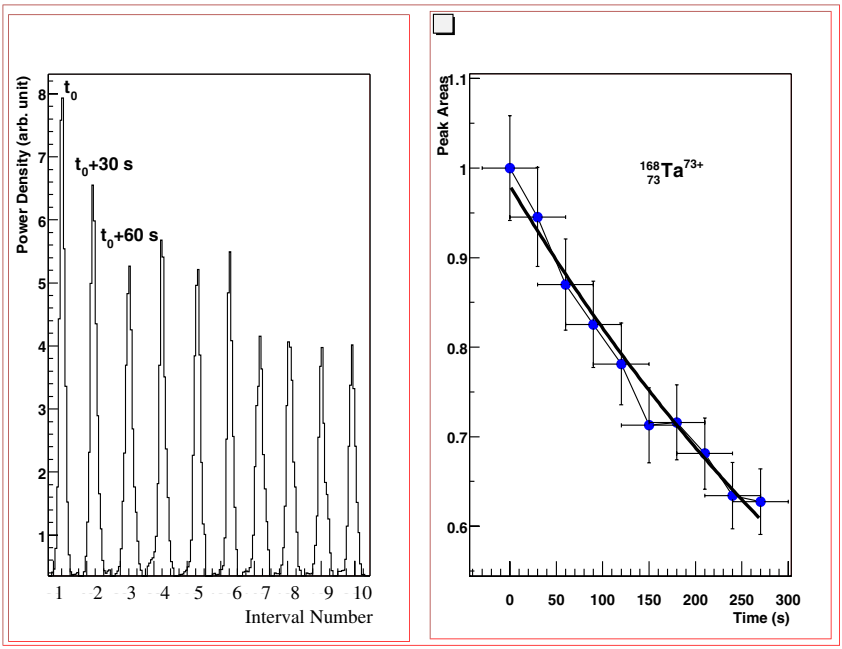

Fig. 13. Lifetime measurement of bare $^{168}Ta^{73+}$ by 'Schottky lifetime spectroscopy'. The left panel shows the Schottky lines of the parent nucleus observed in intervals of 30 s, the right panel the decay curve taken from the corresponding line areas. The extracted half-life in the emitter rest frame (only β^+ decay) amounts, after small corrections for the losses in the ring due to atomic charge changing processes, to $T_{1/2} = 5.2$ min, whereas the half-life of neutral ^{168}Tl is only 2 min (β^+ *and* orbital EC decay). This figure is taken from [28].

both EC and bound-state β^- decays the atomic charge state does *not* change and, therefore, detection of this decay branch by a particle detector is not possible.

Figure 13 shows the result obtained by Schottky lifetime spectroscopy for the case of fast bare ions, where a significant change of β lifetime with respect to the neutral atom was observed [28]. The nucleus ^{168}Ta decays, in the neutral atomic charge state, either by EC or by β^+ decay with comparable probabilities. For bare ^{168}Ta ions, the EC decay channel is 'closed' and only β^+ decay occurs, which roughly triples the lifetime.

4.1 Basics of Bound-State Beta Decay

Nature creates all nuclei beyond iron by neutron capture and β decay in hot stellar plasmas. The more facets of β decay we explore the more we learn on still hidden secrets of both, stellar nucleosynthesis and nuclear structure. This field of research has brought over more than seven decades an incredibly rich harvest of precise data on the one hand, and of theories approaching more and more the very fundaments of weak interaction on the other hand.

Except for very few astronomical observations, our complete knowledge on β decay is due to radioactive bodies found on the earth either, or to nuclei produced by nuclear reactions in terrestrial laboratories. In all these experiments, however, two important properties of *stellar* β decays were missing: the high atomic charge state, due to the high temperature of stellar plasmas, and its counterpart, the huge density of free electrons in the order of 10^{27} cm^{-3} or even more.

The latter, for instance, enables one fundamental step in the hydrogen fusion cycle of the sun and other stars, the β decay of ^{7}Be to ^{7}Li by the capture of *free* electrons. This reaction has never been investigated on the earth, simply because such electron densities are nowhere available. Similarly, β decays, where the 'new' electron will be bound in an (inner) orbit of the daughter atom, instead of leaving it as a free electron, the 'bound-state β^- decay', have not been addressed in the past, simply because the Pauli principle forbids such a process for neutral atoms. For highly ionized atoms of stellar plasmas, however, inner shell vacancies are the rule and not the exception, and thus bound-state β^--decay there becomes a natural decay branch.

Drawing the scheme of nuclear β decay (on the level of nucleons, not quarks) in a symmetric form:

$$n + \nu_e \leftrightarrow p + e^- \tag{8}$$

and taking the particle-antiparticle symmetry into account, five different modes of it can be distinguished:

8.1	$\mathrm{n} + \nu_e$	$\rightarrow \mathrm{p} + \mathrm{e}^-$	β^- continuum decay
8.2	$\mathrm{p} + \nu_e(\mathrm{bar})$	$\rightarrow \mathrm{n} + \mathrm{e}^+$	β^+ decay
8.3	$\mathrm{p} + \mathrm{e}^-(\mathrm{b})$	$\rightarrow \mathrm{n} + \nu_e$	orbital electron capture (EC)
8.4	$\mathrm{p} + \mathrm{e}^-$	$\rightarrow \mathrm{n} + \nu_e$	free electron capture*
8.5	$\mathrm{n} + \nu_e$	$\rightarrow \mathrm{p} + \mathrm{e}^-(\mathrm{b})$	**bound-state β^- decay***

where ν_e, ν_e(bar) denote electron neutrinos and electron antineutrinos, e^-, e^-(b) free and bound electrons, respectively, and asterisks decay modes 'normally' restricted to stellar plasmas. By inverting the arrows, it is easily rec-

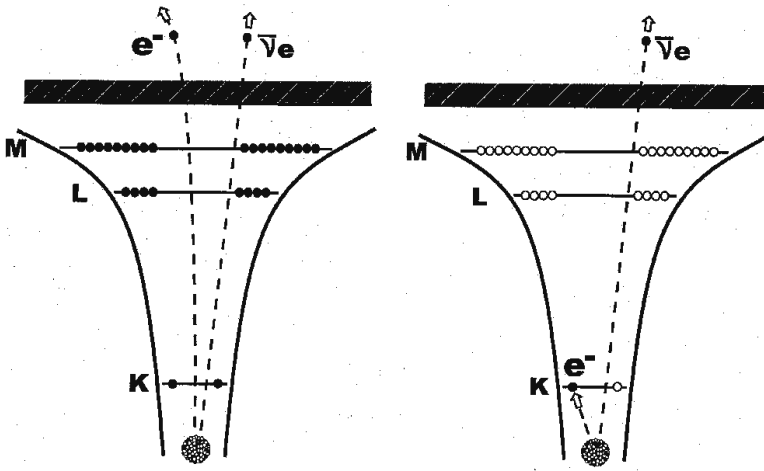

Fig. 14. Continuum β^- decay of a neutral atom (left panel) and bound-state β^- decay of a fully ionized atom to the K shell of the daughter atom, 'saving' the K binding energy (right panel).

ognized that bound-state β^- decay (8.5) is the time-mirrored orbital EC process (8.3), as (8.4) is the time-mirrored counterpart of (8.1). Like orbital EC, bound-state β^- decay is a two-body process, in which the antineutrino carries the total decay energy (Q value) and where the atomic charge state does *not* change (Fig. 14). Only recently, ion storage rings and ion traps provided the first opportunity to store ions in a well-preserved charge state over long times and, thus, to incorporate this hitherto missed fifth decay mode into the list of experimentally investigated β decays.

One of the most intriguing properties of bound-state β^- decay is its higher Q value (energy difference between mother and daughter atom) with respect to neutral atoms. This can be easily understood, because the newly created electron does not leave the attractive Coulomb potential of the nucleus and 'saves' its binding energy in the daughter atom. Hence, in first order, the Q values of continuum- and bound-state β^- decay just differ by the electron binding energy. An exact calculation has to consider that the Q value for continuum β^- decay is defined as energy (mass) difference of the neutral mother atom with nuclear charge Z (M_Z) on the one hand and the singly charged daughter atom with nuclear charge (Z+1) and an electron at rest ($M_{Z+1} + m_e$) on the other hand. Bound-state β^- decay, however, occurs for highly charged ions only. Taking this into account, one gets the following relation between the Q values for the continuum β^- decay of a neutral atom ($Q_{\beta c}$) and the bound-state decay of the corresponding *bare* atom $Q_{\beta b}$ [32]:

$$Q_{\beta b} = Q_{\beta c} - |\Delta B_e| + |B_e^{K,L\cdots}| \tag{9}$$

where $|\Delta B_e|$ denotes the difference of the sum of all electron binding energies of the neutral mother- and daughter-atom, respectively, and $\left|B_e^{K,L\cdots}\right|$ the binding energy of the new electron depending on its 'birthplace' in the K or L....shell of the daughter atom. Equation (9) has to be slightly modified when considering bound-state β^- decay of hydrogen-like or helium-like ions.

A negative value of $Q_{\beta c}$ indicates that an atom is β-stable in the neutral atomic charge state. However, when the difference $\left|B_e^{K,L\cdots}\right| - |\Delta B_e|$ exceeds the absolute value of a negative $Q_{\beta c}$, it gets unstable with respect to bound-state β^- decay, if (almost) all of its electrons are stripped off. In the first observation of bound-state β^- decay such a case has been addressed: ^{163}Dy is stable as a neutral atom, but decays as a *bare* ion to ^{163}Ho by bound-state β^- decay. The half-life of bare ^{163}Dy ions, measured at the ESR, amounts to only 47 days [32].

The pathway of the s-process of nucleosynthesis near the valley of β stability is determined by a subtle balance of neutron capture and β lifetimes. Since with increasing temperature the mean ionic charge state gets larger, bound-state β^- decay probabilities are growing and, thus, β lifetimes will be reduced. This may lead to an increasing number of branching points in the s-process pathway. If one knows at those points the bound-state β^- decay-strengths for the relevant atomic charge states, one can determine from the observed branching ratios the corresponding temperatures, when assuming, for instance, a relation between charge-state distribution and temperature according to the Saha equation. In most cases, bound-state β strengths can be calculated rather precisely for known probabilities of the corresponding continuum decays, i.e. for known nuclear matrix elements [33]. There are a few, but important cases, however, where bound-state β^- decay opens, due to the enlarged Q value, a decay channel that is forbidden for the neutral atom. Among those decays with unknown nuclear matrix element are ^{205}Tl, which might serve as a detector for solar pp-neutrinos with a threshold of only 60 keV, or ^{187}Re that will be discussed next.

4.2 Bound-State Beta Decay of Bare ^{187}Re and the Age of the Universe

Thoughts on the size, the origin and the fate of the universe belong to mankind since the earliest steps towards human culture many ten thousand years ago. Quite recently, this never interrupted thinking received new fuel by observations that might suggest the existence of a puzzling 'cosmological constant', of 'dark energy' and of a faster and faster expanding universe [34].

The mathematical basis for those conclusions are the Friedmann–Lemaitre equations, that were derived from Einstein's field equations of General Relativity under the assumption of a homogeneous and isotropic universe. A closer inspection of these equations shows that strong constraints for matter density, geometry and cosmological constant can be provided by generally accessible 'observables', in particular by today's Hubble constant H_0, and by

the age T_U of the universe [35]. Observation-based numbers for both, H_0 and T_U are, therefore, mandatory to put — what yet are speculations — on a safe ground.

There are two distinct approaches to get limits for the (minimum) age of the universe: the first one is based on astronomical observations, the second one on nuclear 'eon clocks'. The former method mainly focuses on the determination of the age of the oldest stars in our galaxy, such as found in globular clusters of the galactic halo. Collecting a wealth of data, the uncertainties could be more and more narrowed: to date an age for the oldest observed globular clusters of $(12 \pm 2) \times 10^9$ years is commonly accepted [36]. This number represents a fortiori also a lower limit for T_U, the age of the universe.

However, because the time scale of this method depends on the underlying *assumed* time scales of stellar evolution, it is highly desirable to have a thoroughly independent access to T_U. That was found in nuclear 'eon clocks'. The age of our solar system and of the earth has been determined to $(4.56 \pm 0.04) \times 10^9$ y, with an incredibly small uncertainty of less than one percent by means of long-lived radioactive couples, as found in meteorites, rocks or in the oceans [37]. To derive the age of these bodies, one has to measure in principle only the present abundance ratio of mother and daughter nuclei, and to know the α- or β-decay probability of the mother. The most widely used nuclear clocks in this context are: $^{40}K/^{40}Ar$ (β-decay; $T_{1/2} = 1.3 \times 10^9$ y); $^{87}Rb/^{87}Sr$ (β-decay; $T_{1/2} = 50 \times 10^9$ y); $^{238}U/^{232}Th$ (α- and β-decay chains; $T_{1/2} = 4.5 \times 10^9$ y (U), $T_{1/2} = 14.5 \times 10^9$ y(Th)); $^{176}Lu/^{176}Hf$ (β decay; $T_{1/2} = 30 \times 10^9$ y), and $^{187}Re/^{187}Os$ (β-decay; $T_{1/2} = 42 \times 10^9$ y) [38].

It was near at hand to estimate by this method also the age of our galaxy *before* the decoupling of the solar system. Very encouraging was the proof of Symbalisty and Schramm [39] that alone from the abundance ratio and the decay constant of present bodies the age of our pre-solar galaxy can be figured out within a factor of two, independent on the number of supernovae, by which these bodies were formed or recycled. It turned out, that the obviously best suited clock for this purpose is the $^{187}Re/^{187}Os$-couple. All other potential clocks show serious problems: they are not long-lived enough ($^{40}K/^{40}Ar$); or, their production process is not fully understood (s- and/or r-process in case of $^{87}Rb/^{87}Sr$); or, they have isomeric states that can become thermally excited in a hot environment and then might decay in a short time ($^{176}Lu/^{176}Hf$); or they do not belong to the same decay chain ($^{23}8U/^{232}Th$), which demands additional assumptions on their relative production probability in the r-process.

Takahashi and Yokoi yielded from the $^{187}Re/^{187}Os$ clock — in the framework of the Schramm-Wasserburg model — a total age T_G of our galaxy (including the age of the solar system) of 14×10^9 y $< T_G < 28 \times 10^9$ y, i.e. also a lower limit for the age of the universe as $T_U > 14 \times 10^9$ y [40]. Lateron Takahashi pointed out [41] that these numbers could be entirely

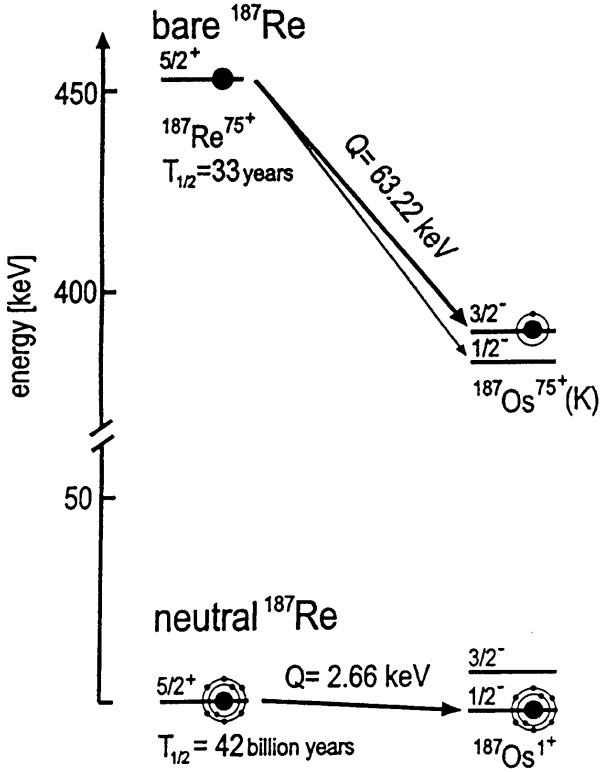

Fig. 15. β-decay schemes for neutral (bottom) and fully ionized ^{187}Re (top). For *neutral* ^{187}Re only the unique, first forbidden transition to the ^{187}Os *ground state* is energetically possible. Together with the small nuclear matrix element, the small Q value lead to a halflife of 42 x 10^9 y. For *fully ionized* ^{187}Re the continuum β^- decay is forbidden (negative Q value), whereas bound-state β^- decay with the electron bound in the K shell becomes possible. The dominant decay branch, a nonunique first forbidden transition, feeds the *first excited state* in ^{187}Os at 9.75 keV excitation energy. This effect dramatically decreases the half-life of bare ^{187}Re, as measured at the ESR (see next section), to 33 y only. The figure is taken from [42].

wrong, because in the course of galactic history ^{187}Re would be once or several times recycled into a stellar environment getting highly ionized there. Then a bound-state β^- decay to the first excited state at 9.75 keV of ^{187}Os could take place (Fig. 15), which is not accessible in the decay of neutral ^{187}Re ($Q_{\beta c} = 2.6$ keV). The unknown nuclear matrix element of this transition can be determined only by measuring the bound-state β^- decay of bare or hydrogenlike ^{187}Re. By a first estimate, based on Q value, spin and parity of this transition, Takahashi predicted for *bare* ^{187}Re a half-life of 14 years that is by more than *nine orders of magnitude shorter* than the half-life of

42 x 10^9 y for neutral ^{187}Re! This prediction was challenging enough to be proven or disproved by an ESR experiment. If Takahashi's estimate would be only roughly correct, the reliability of the ^{187}Re/^{187}Os eon clock would become doubtful, to say the least.

Half-life determination of $^{187}Re^{75+}$ and its virtue as an 'eon clock'. Provided that a high-energy accelerator and an ion storage-cooler ring are available, the half-life determination of fully ionized ^{187}Re — with a presumed value of a few ten years — becomes conceptually rather simple, because ^{187}Re as a quasi–stable atom can be provided by a 'normal' ion source and then, after acceleration to an energy of about 400 AMeV, fully stripped and injected into the storage-cooler ring. There, the cooled mother ions circulate with preserved atomic charge state for some hours, and, thus, the bound β decay-constant, $\lambda_{\beta b}$, can be determined from the number of daughter ions growing in linear proportion to the storage time. In an ideal case, these daughters would be directly accessible in a Schottky line, well-resolved from the mother ions.

In the actual case [42] this simple technique could not be applied, however, since the Schottky lines of the bare mother $^{187}Re^{75+}$ and the hydrogen-like daughter ions $^{187}Os^{75+}$ were *not* resolved, due to the small Q value of only 63 keV. Therefore, after an extended storage time an internal gas jet of argon ions was turned on, intercepting the stored ions at right angle and stripping off the one electron of the $^{187}Os^{75+}$ ions within a time of about 2 min, that is very short with respect to the storage time. Thus, the *bare* $^{187}Os^{76+}$ ions, showing a different trajectory and revolution frequency, could be easily detected, either as well-resolved Schottky line (Fig. 16) or by means of a detector positioned at an appropriate place in the ring aperture. The amount of bare ^{187}Os ions, generated by nuclear reactions in the gas jet, was determined in experiments with very short storage times. For typical numbers of 10^8 stored primary bare ^{187}Re ions, a few hundred ^{187}Os ions per hour were generated. From those numbers the impressively short half-life of 33 years for bare ^{187}Re has been determined.

From the measured half-life of bare ^{187}Re and its error the previously unknown nuclear matrix element for the β decay to the first excited state of ^{187}Os was extracted, yielding a log ft-value of (7.87 ± 0.03) for this transition. Therewith, the lifetimes for all atomic charge states q^+ of $^{187}Re^{q+}$ can be safely calculated.

As outlined above, from all potential nuclear 'eon clocks' the ^{187}Re/^{187}Os couple should have the most reliable clockwork providing constraints for the age of our galaxy that are strictly independent on astronomical models describing galactic and stellar evolution. The most important result of the experiment described above is, however, that the half-life of ^{187}Re gets dramatically dependent on its atomic charge state.

Therefore, it is no longer possible to extract constraints for the age of our galaxy just from the two numbers, the ^{187}Re/^{187}Os abundance on the one

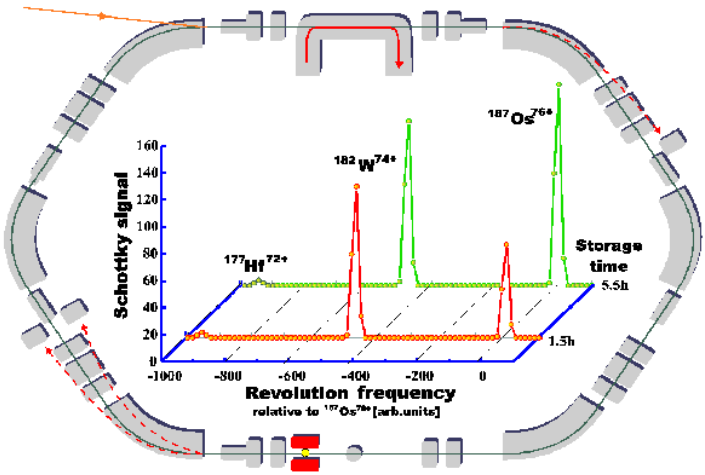

Fig. 16. Schottky spectra of stored ions after operation of the internal gas jet (the very strong line of primary bare ^{187}Re ions is not shown) for storage times of 1.5 h and 5.5 h, respectively. The number of bare ^{187}Os ions, due to bound-state β^- decay, grows in proportion to the storage time, whereas the amount of ^{177}Hf and ^{182}W nuclei, due to nuclear reactions in the internal gas target, is independent on it.

hand, and 'the' decay constant λ_{Re} of ^{187}Re on the other hand. Rather, one has to substitute λ_{Re} by an *effective decay constant* $< \lambda_{Re}$ (q) $>$, properly weighted over all the atomic charge state dependent decay constants λ_{Re}(q). To get this effective decay constant it becomes indispensable, however, to re-draw the galactic life- story of a typical ^{187}Re atom, i.e.to figure out how often it was re-astrated in the average, where and how long it experienced several temperatures (charge states) in the different stellar environments during its galactic encounters. Therewith, the initially supposed *independence* of the ^{187}Re eon clock from any uncertainties and peculiarities of galactic evolution models is *lost*.

It remains 'allowed', of course, to try such a galactic life-story of ^{187}Re in the framework of current stellar evolution models, but now based on its *known* decay constants λ_{Re}(q). Proceeding in this way, Takahashi and Arnould obtained a value of $T_G = (13.5 \pm 4)$ x 10^9 y for the age of our galaxy from the 'rescaled' ^{187}Re clock [43], which reasonably well fits to the value of $T_G = (12 \pm 2)$ x 10^9 y, as obtained from the oldest globular clusters. One should be aware, however, that the clockworks of these two 'clocks' are now *basically intertwined*, in contrast to the initially intended idea.

4.3 Measurement of a Continuum and Bound-State Branching Ratio

Since decades, for a wealth of atomic nuclei the ratio of orbital EC and of continuum β^+ decay is well known both experimentally and theoretically [44]. This branching reflects the relative strength of the Coulomb wave function of the positron as created in the continuum β^+ decay on the one hand, and of the wave function of the bound electron as annihilated in the orbital EC on the other hand. However, the corresponding ratio of the time-mirrored processes, β^- transitions to a bound or, respectively, a continuum electron state, could be evaluated so far only theoretically. Although the advent of ion storage–cooler rings helped to overcome this problem, and although bound-state β^- decay could be detected in the ESR for the first time at the examples of bare ^{163}Dy and bare ^{187}Re, no branching ratio of bound and continuum β^- transitions had been measured so far. Concerning the experiments mentioned above, this was impossible for the simple reason that for either nucleus investigated there only bound, but no continuum β^- decay is allowed energetically.

Quite recently, such a branching ratio has been measured for the first time at the examples of bare $^{207}Tl^{81+}$ and $^{206}Tl^{81+}$ ions, respectively, that were stored and cooled in the ESR. In these cases both, continuum and bound-state β^- decay are energetically allowed. Moreover, due to the rather large Q values of about 1.5 MeV for bound-state β^- decay the Schottky lines of mother and daughter atoms, respectively, do appear well-resolved. From the time dependent areas of these lines the total and bound-state decay constants can be determined, respectively, and, hence, the bound-to-continuum branching ratio. The data evaluation is still in progress. Figure 17 shows, for the case of ^{206}Tl, the Schottky traces of a ^{206}Tl isomer, the ^{206}Tl ground state and of its bound-beta daughter, ^{206}Pb, as a function of time after injection of the ^{206}Tl fragments into the ESR. In particular the high resolution (80 Hz at 60 MHz), and the 'direct' access to the corresponding Q values should be emphasized.

5 Summary and Outlook

Ion storage–cooler rings, fed by unstable nuclei, have been proven as excellent tools to address the ground state properties of them, such as mass and (β lifetime. Their mass resolving power $m/\Delta m$ in the order of 10^6 is rather high and certainly sufficient for most purposes, but will never compete with 'world records' obtainable in ion traps in the regime of stable nuclei. On the other hand, cooler rings are unsurpassed to date concerning their 'effectivity', i.e. the capability to measure simultaneously many dozens of masses, and their ultimate sensitivity down to one single stored (highly charged) ion. Furthermore, the complementary techniques of Schottky- and of isochronous mass spectrometry allow to cover the entire range of interesting β lifetimes, from the sub-millisecond region to hundreds of years. Cooler rings also provided

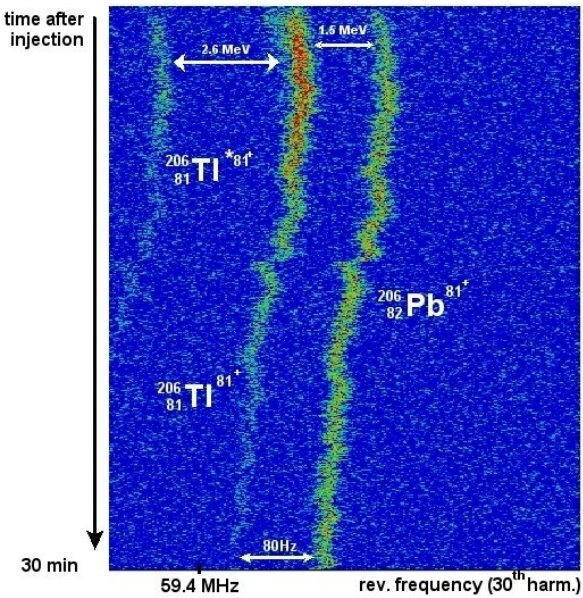

Fig. 17. Time–traces of Schottky lines vs. the 30th harmonics of the revolution frequencies (about 60 MHz) of stored and electron-cooled bare ^{206}Tl ions. From left to right: short-lived isomeric state of $^{206}Tl^{81+}$ at 2.6 MeV excitation energy; $^{206}Tl^{81+}$ ground state; bound β daughter of it, hydrogen-like $^{206}Pb^{81+}$. The (parallel) fluctuations of a few Hz in the revolution frequencies are due to random jitters of magnetic fields and power supplies.

the very first opportunity to address some exotic β decay modes of hot stellar plasmas, such as bound-state β^- decay.

In the future, cooler rings will remain the indispensable 'working horses' for mass- and lifetime mapping of nuclei far from stability. However, to reach the key nuclei of explosive nucleosynthesis of both the r- and rp-processes, first of all a significant improvement of the intensity of secondary beams is necessary. What is yet a challenge will hopefully become soon reality by the advent of the new facilities, such as the planned secondary beam factory at GSI [45].

Acknowledgment

This contribution is entirely based on the work and on previous publications of my colleagues of the FRS–ESR mass group. To all of them I am deeply obliged: F. Attallah, K. Beckert, K.H. Behr, P. Beller, D. Boutin, L. Chulkov, Th. Faestermann, M. Falch, B. Franczak, B. Franzke, H. Geissel, M. Hausmann, M. Heillström, E. Kaza, Th. Kerscher, P. Kienle, O. Klepper, H.-J. Kluge, Ch. Kozhuharov, Yu.A. Litvinov, K.E.G. Löbner, L. Maier,

M. Matos, G. Münzenberg, F. Nolden, Yu.N. Novikov, T. Ohtsubo, M. Portillo, T. Radon, Ch. Scheidenberger, J. Stadlmann, M. Steck, K. Sümmerer, K. Takahashi, Th. Stöhlker, H. Weick, M. Winkler, H. Wollnik and T. Yamaguchi. I thank M. Steck, who kindly provided me with some figures. The help of S. Lüttges concerning style, grammar and typing is acknowledged as well as C. Hoelzer's support in transforming the figures to their final form.

References

1. B. Franzke: Nucl. Instr. Meth. B **24**, 18 (1987)
2. H. Geissel et al.: Nucl. Instr. Meth. B **70**, 247 (1992)
3. W. Magnus, S. Winkler: *'Hills Equations'*, Dover, New York (1979)
4. D. Nesvorny et al.: Asteroids **III**, 379 (2002)
5. H. Wu: *'Complex Analysis III'*, Lectures Notes in Math., Springer, Berlin (1987)
6. H.J. Metcalf, P. van de Straten: *'Laser Cooling an Trapping'*, Springer, New York (1999)
7. M.H. Anderson et al.: Science **269**, 198 (1995)
8. D. Habs, R. Grimm: Ann. Rev. Nucl. Part. Sci. **45**, 391 (1995)
9. I. Klaft et al.: Phys. Rev. Lett. **73**, 2425 (1994)
10. S. van der Meer: Nobel lecture 1984, in: Les Prix Nobel **1984**, ed. Nobel Foundation, p. 102
11. F. Nolden: private communication
12. M. Steck: J. Opt. Soc. America B **20** no. **5**, 1016 (2002)
13. G.I. Budker: At. Energy **22**, 346 (1967)
14. G.I. Budker in: 'Proc. of the Int. Symp. on Electron and Positron Storage Rings', Saclay 1966, eds. H. Zyngier and E. Crémieux-Alean: PUF, Paris (1967), II-1-1, pp. 1–15
15. H. Poth: *'Electron cooling. theory, experiment, application'*, in: Phys. Rep. **196**, 135 (1990)
16. H. Danared et al.: Phys. Rev. Lett. **72**, 3775 (1994)
17. M. Steck et al.: Phys. Rev. Lett. **77**, 3803 (1996)
18. E.M. Burbidge, G.R. Burbidge, W.A. Fowler, F. Hoyle: Rev. Mod. Phys. **29**, 547 (1957)
19. Z.Y. Bao, F. Käppeler: Atomic Data Nucl. Data Tables **26**, 411 (1987)
20. C. Freiburghaus et al.: Astrophys. J. **516**, 381 (1999)
21. H. Schatz et al.: Phys. Rep. **294**, 167 (1998)
22. F. Käppeler, F.-K. Thielemann, M. Wiescher: Ann. Rev. Nucl. Part. Sci. **48**, 175 (1999)
23. B. Pfeiffer, K.-L. Kratz, F.K. Thielemann: Z. Phys. A **357**, 235 (1997)
24. D.J. Morrissey, B.M. Sherrill: In-Flight Separation of Projectile Fragments, Lect. Notes Phys. **651**, 113–135 (2004)
25. H. Geissel et al.: Nucl. Phys. A **701**, 259c (2002)
26. C. Scheidenberger: private communication
27. T. Radon et al.: Nucl. Phys. A **677**, 75 (2000)
28. F. Attallah et al.: Nucl. Phys. A **701**, 561c (2002)
29. M. Hausmann et al.: Nucl. Instr. Meth. A **446**, 569 (2000)
30. Yu.A. Litvinov et al.: Hyperfine Interactions **132**, 283 (2001)
31. J. Stadlmann et al. in: Proc. STORI99, AIP Conf. Proc. **512**, 305 (2000)

32. M. Jung et al.: Phys. Rev. Lett. **69**, 2164 (1992)
33. K. Takahashi, K. Yokoi: Atomic Data Nucl. Data Tables **26**, 375 (1987)
34. S. Perlmutter et al.: Astrophys. J. **517**, 565 (1999); J. Glanz. Science **282** (1998)
35. F. Bosch: *'Rhenium-187 and the age of the galaxy'* in: AIP Conf. Proc. **477**, 16 (1999); and ICAP, Windsor, Canada, 1998, ed. by W.E. Baylis, G.W.F. Drake, pp. 344–360
36. D.A. Vandenberg et al.: Ann. Rev. Astron. and Astrophys. **34**, 461 (1996)
37. E. Anders et al.: Geochim. Cosmochim. Acta **53**, 197 (1989)
38. K. Yokoi, K. Takahashi, M. Arnould: Astron. and Astrophys. J. **117**, 65 (1983)
39. E.M.D. Symbalisty, D.N. Schramm: Rep. Prog. Phys. **44**, 293 (1981)
40. K. Takahashi, K. Yokoi: Nucl. Phys. A **404**, 578 (1983)
41. K. Takahashi, K. Yokoi: Phys. Rev. C **36**, 1522 (1987)
42. F. Bosch et al.: Phys. Rev. Lett **77**, 5170 (1996)
43. K. Takahashi: *'The* ^{187}*Re-*^{187}*Os cosmochromometry and chemical evolution in the solar neighborhood'*, in: Tours Symp. on Nucl. Phys. III, ed. by M. Arnould et al., AIP Conf. Proc. **425**, 616 (1997)
44. H. Behrens, J. Jaenecke: *'Numerical Tables for β-Decay and Electron Capture'*, Landolt-Börnstein, New Series GG1, Vol. **4** (2001)
45. W.F. Henning: *'Conceptional Design Report'*, unpublished, GSI (2001) http://www.gsi.de/GSI-future/cdr/